Chemical Physics Letters 871 (2025) 142095

Contents lists available at ScienceDirect

Chemical Physics Letters

journal homepage: www.elsevier.com/locate/cplett

Research paper

Ultrafast ring-opening dynamics of 1,2-dithiane following ultraviolet absorption

Patrick A. Robertson [b], James Merrick [a], David Heathcote [a], Matthew S. Robinson [c], Alexander Butler [a], Yasmine Biddick [a], J.F. Pedro Nunes [d], Conor Rankine [e], Zhihao Liu [a], Samuel F. Arrowsmith [a], James O.F. Thompson [f], M. Nrisimha Murty [f], Richard Chapman [f], Emma Springate [f], Edward A. Anderson [a], Adam Kirrander [a], Claire Vallance [a,*]

[a] Department of Chemistry, University of Oxford, Chemistry Research Laboratory, 12 Mansfield Rd, Oxford OX1 3TA, UK
[b] School of Chemistry, University of Nottingham, Nottingham, UK
[c] European XFEL, Schenefeld, Germany
[d] Diamond Light Source, Harwell, UK
[e] Department of Chemistry, University of York, UK
[f] Central Laser Facility, Rutherford Appleton Laboratory, Harwell, UK

GRAPHICAL ABSTRACT

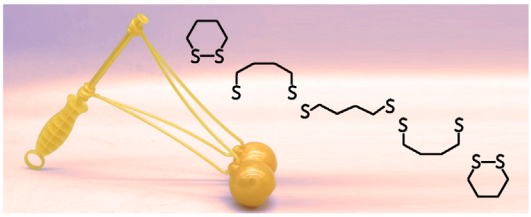

Ultrafast pump-probe measurements allow observation of the photoinduced molecular clackers motion in 1,2-dithiane.

HIGHLIGHTS

- Time-resolved mass spectrometry is sensitive to ultrafast nuclear dynamics.
- 1,2-dithiane is a small-molecule model for a disulphide bond.
- Photoexcitation initiates intriguing dynamics over multiple electronic surfaces.
- Trajectory surface hopping calculations offer insight into the experimental results.

ARTICLE INFO

Keywords:
1,2-dithiane
Ultrafast dynamics
Nonadiabatic dynamics
Time-resolved mass spectrometry
Trajectory surface hopping

ABSTRACT

We report results from a recent laser pump–probe study into the ultrafast ring-opening dynamics of 1,2-dithiane. Following absorption of a 290 nm photon, the nuclear dynamics were probed as a function of pump–probe delay on the femtosecond timescale by strong-field ionisation with an 800 nm probe pulse, resulting in production of a range of atomic and molecular fragment ions. The time-dependent yields of atomic fragment ions reveal evidence of coherent nuclear wavepacket dynamics corresponding to the previously proposed 'Newton's cradle' motion of 1,2-dithiane, in which repeated ring opening, structural inversion, and ring closing occurs on a timescale of ~400-500 fs. Based on surface-hopping trajectory simulations of the non-adiabatic dynamics, we are able to rationalise the observed time-dependent ion yields in terms of a geometry-dependent variation in ionisation energy for the photoexcited 1,2-dithiane molecule.

* Corresponding author.
E-mail address: claire.vallance@chem.ox.ac.uk (C. Vallance).

https://doi.org/10.1016/j.cplett.2025.142095
Received 8 February 2025; Received in revised form 21 March 2025; Accepted 13 April 2025
Available online 30 April 2025

1. Introduction

1,2-dithiane is a six-membered heterocyclic compound containing a disulphide bond. It can be considered a model for a disulphide bridge, an important functional group which helps to define and stabilise tertiary structure in peptides and proteins [1,2]. There has been considerable interest in 1,2-dithiane, both from an experimental and a theoretical point of view, due to the novel dynamics it exhibits in the gas phase upon photoexcitation with ultraviolet (UV) light [2–9]. While disulphide bonds are not inherently photochemically stable, and cleave readily on a timescale of a few tens of femtoseconds following UV excitation, these investigations into the detailed photodynamics of 1,2-dithiane reveal a potential photoprotective mechanism in which the S–S bond may re-form on a timescale of a few picoseconds. This is well matched with accessible timescales for ultrafast structural techniques, and 1,2-dithiane has subsequently become an interesting test case for such methods.

Coulomb-explosion imaging has been shown by a number of authors (see for example [10–15]) to be a useful probe of evolving molecular structure on the femtosecond timescale. The approach is based on the assumption that if a sufficiently large number of valence electrons can be removed from a molecule on a timescale faster than molecular vibration – typically achieved either *via* core–shell X-ray ionisation or by strong-field ionisation – the resulting Coulomb explosion will map the initial atomic positions onto the final velocities of the recoiling ions. By measuring these final velocities using velocity-map imaging or a related technique, one can in principle reconstruct the initial molecular structure.

In the present study, to probe the evolving molecular structure of 1,2-dithiane following UV photoexcitation we perform a simpler version of Coulomb explosion imaging, namely Coulomb explosion time-of-flight mass spectrometry. This approach exploits the fact that not only the final ion velocities, but also the ionisation probability and therefore the total ion yields, are sensitive to the molecular structure. We report results from pump–probe experiments in which 1,2-dithiane is photoexcited in the gas phase at 290 nm and the products are probed via strong-field ionisation, with the photoionisation products detected via time-of-flight mass spectrometry on the femtosecond to picosecond timescale.

2. Methods

2.1. Experiments

Experiments were performed on the AMO end station [16] at the Artemis ultrafast laser facility, which forms part of the Central Laser Facility at the UK's Rutherford Appleton Laboratory.

1,2-dithiane (hereafter simply referred to as 'dithiane') was synthesised according to the methods of Singh and Whitesides [17] (see SI for further details). Dithiane has a melting point of 32.5 °C (305.5 K), and is therefore a solid at room temperature. To prepare the molecule in the gas phase, the gas line was heated to around 37 °C (~310 K), and the vapour pressure was used to form a continuous effusive molecular beam, which entered the extraction region of the time-of-flight spectrometer. The base pressure in the experimental chamber was ~8×10^{-8} mbar with the beam off, rising to ~5×10^{-7} mbar with the beam on. Based on signal levels and sample lifetime, the sample density in the interaction region was estimated to be around 10^{13} molecules cm^{-3}.

Within the extraction region, the molecular beam was crossed with the pump and probe laser beams. The 10 μJ, ~150 fs FWHM, 290 nm pump pulses were generated by an optical parametric amplifier and focused down to a spot size of ~100 μm at the intersection with the molecular beam. The ~300 μJ, ~40 fs, 800 nm probe pulses were tightly focused to a spot size of ~25 μm in the interaction region, yielding an intensity of over 10^{15} W cm^{-2}, sufficient to cause strong-field ionisation of the photoexcited dithiane molecules (Keldysh parameter $\gamma \leq 0.25$). The cross-correlation time for the two laser pulses was measured to be in the range 150–200 fs over the course of the beamtime (the precise value was treated as a fitting parameter during our data analysis - see Section 3), and the pump–probe delay was scanned over a range from approximately −500 to 1000 fs.

Ions formed in the interaction region were accelerated by an electric field along the time-of-flight tube to a position-sensitive detector comprising a pair of 75 mm microchannel plates coupled to a P47 phosphor screen. Each incoming ion generated a flash of light on the phosphor, which was imaged by a second-generation Pixel Imaging Mass Spectrometry (PImMS2) camera, yielding an (x, y, t) data point for each detected ion. In practice, each ion generally illuminates multiple pixels and time bins within the PImMS2 sensor. A centroiding algorithm is employed to reduce each ion signal to a single (x, y, t) data point, improving the spatial and temporal resolution and also reducing the size of the data set. Integrating the data set recorded for each pump–probe delay over the x and y coordinates yielded the photofragment time-of-flight spectrum for that delay time.

The experiment was run at a repetition rate of 20 Hz, limited by the maximum readout rate of the PImMS2 camera.

2.2. Electronic structure calculations

In order to explore how the variation in nuclear structure may affect the ionisation potentials (IPs) of dithiane, and subsequently, how this may rationalise the ion yields of sulphur-containing fragment ions, ionisation potentials were calculated at multiple time points along a subset of trajectories which were sampled from previous nonadiabatic dynamics simulations of dithiane. Simulations employed the trajectory surface hopping (TSH) method with Tully's fewest-switches algorithm [18], and were performed using the SHARC (version 2.1) software package [19–21] interfaced with the OpenMolcas v23.02 electronic structure program [22]. Electronic structure calculations were performed at the SA(4|4)-CASSCF(6,4)/ANO-R1(t) level of theory [23,24], where SA(4|4) denotes state-averaging over the four lowest-energy singlet and triplet states, and ANO-R1(t) refers to a truncated ANO-R1 basis set where superfluous polarisation functions on hydrogen atoms were removed. Trajectories were propagated for 1 ps with a nuclear propagation timestep of 0.5 fs. Full computational details regarding the TSH simulations can be found in the SI, and a comprehensive examination of the TSH simulations performed in this study will be the focus of an upcoming publication [25].

From a total ensemble of 384 TSH trajectories, a subset of 50 representative trajectories were selected by random sampling for the ionisation potential calculations. To check that the subset of trajectories was suitably representative of the complete set, the average values of the S–S distance across each of the two trajectory sets were compared, and found to match almost identically. Convergence tests were performed with between 10 and 50 trajectories to ensure that 50 trajectories were sufficient to model the behaviour of interest. Further details of these tests can be found in the SI.

For each trajectory, the molecular geometries at every 50 fs time interval were extracted. Single-point electronic structure calculations were then performed on each geometry at the SA(4|4)-CASSCF(6-n,4)/ANO-R1(t) level of theory, where n = (0, 1, 2, 3) for calculating neutral, 1+, 2+ and 3+ charge states respectively. For simplicity, only singlet electronic states were considered for charge states with an even number of electrons (0 and 2+), and only doublet electronic states were considered for charge states with an odd number of electrons (1+ and 3+). The ionisation potentials were then calculated simply as the difference in state energies at each time step, and averaged over all 50 trajectories.

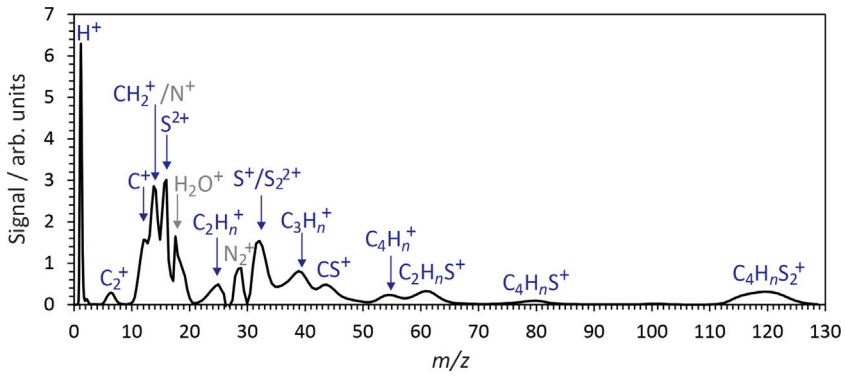

Fig. 1. Background-subtracted time-of-flight mass spectrum of fragment ions formed in the Coulomb explosion initiated by strong-field ionisation of 1,2-dithiane by the ~10^{15} W cm^{-2}, 800 nm probe laser. Peaks arising from residual background N_2 and H_2O present in the vacuum system and/or gas sample is labelled in grey.

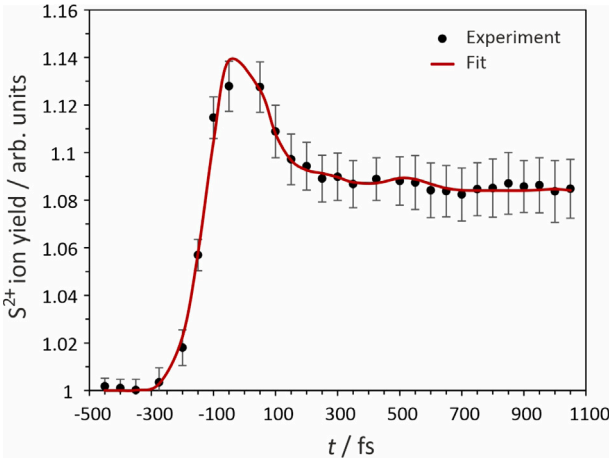

Fig. 2. Signal observed in the m/z 16 (S^{2+}) mass channel following 290 nm photoexcitation of 1,2-dithiane, plotted as a function of pump–probe delay. The fit to the data (see text for details) is shown in red.

To enable comparison between the predictions of the simulations and the experimental data, the resulting time-dependent functions were convoluted with a Gaussian with a full-width half maximum equal to 190 fs in order to account for the cross-correlation time between the pump and probe laser pulses.

3. Results and discussion

Before presenting the time-resolved (pump–probe) data, we first consider the time-of-flight mass spectrum recorded in a probe-only measurement. In this case there is no photoexcitation step, and the probe laser induces (single and multiple) ionisation of ground-state dithiane at its equilibrium geometry. The resulting mass spectrum, recorded with a probe laser power of ~10^{15} W cm^{-2}, is shown in Fig. 1.

We note that Artemis end station used to record the data in the present study was designed for photoelectron imaging, and as a result has a rather short flight tube which unfortunately placed significant limitations on the achievable m/z resolution. Nonetheless, under the high laser intensity conditions employed, we observe a variety of atomic and molecular fragments. Several of the largest signals arise from atomic ions, indicating that for at least a significant subset of molecules we achieve almost complete Coulomb explosion into atomic ions.

We now move on to consider the time-dependent pump–probe data. The clearest hallmark of the photoinduced dynamics is found in the m/z = 16 mass channel, which corresponds to S^{2+} ions[1] The total ion signal in this mass channel is shown as a function of pump–probe delay in Fig. 2 (black circles), together with two-standard-deviation uncertainties. The figure also shows a fit to the data (red line), which will be discussed later. At negative pump–probe delays, when the 800 nm probe laser pulse arrives at the interaction region before the 290 nm pump laser pulse, we see S^{2+} signal arising from strong-field ionisation of ground-state dithiane. At the point where the two laser pulses are coincident in time (t = 0) in Fig. 2, we observe a rapid rise in signal, followed by first a rapid decay over the first few hundred fs, and then a much slower decay overlaid with an oscillation which persists until the end of the measurement, completing two full cycles.

The time dependent signal observed in our experiments is very similar to that observed previously by Stephansen et al. [2] in another time-dependent mass spectrometry study of dithiane following 284 nm photoexcitation. In their case the photoexcitation products were probed via 400 nm multi-photon single ionisation. In contrast to our strong-field ionisation study, in which most of the observed fragments are atomic, Stephansen and coworkers observed two major ions: the parent ion at m/z 120; and the $C_4H_7^+$ ion at m/z 55, with the latter the product of S_2H loss from the parent ion. The time-dependent ion yield for the m/z 55 fragment has many features in common with that observed for the S^{2+} ion in the present study, though the oscillatory component of the signal appears to be damped more rapidly.

Stephansen et al. fit their time-dependent data for $t > 0$ to a kinetic model containing two exponential decays with time constants τ_1 and τ_2, and an oscillating component with frequency ω and phase ϕ. The initial ultrafast decay, which was found to occur on a timescale of <200 fs (τ_1 = 177 ± 17 fs), was interpreted as corresponding to the S–S bond stretching on the S_1 excited-state surface to reach the minimum energy configuration on this surface. The oscillatory component of the signal was interpreted in terms of a 'wiggling motion' of the carbon backbone near the minimum energy region on the S_1 state which causes the S–S bond distance to oscillate, with a peak in the signal observed when the two sulphur atoms are at their closest separation and a valley at larger separations. The oscillation period of 411 ± 27 fs determined from the fit to the experimental data agreed with the 416 fs period predicted by quantum mechanical calculations. Finally, the decay of the signal over longer timescales was explained by passage through the S_1-S_0 conical intersection, which lies in the vicinity of the S_1 minimum, resulting in re-formation of the S–S bond on the ground state. The resulting intact

[1] We note that there may also be a small contribution to the m/z16 signal from O^+ ions arising from background O_2 in the vacuum system. This background signal should mostly be removed by the background-subtraction process, but since O_2 does not absorb significantly at 290 nm, any residual contribution is expected to manifest as a constant time-independent background and therefore does not affect any of our S^{2+} results.

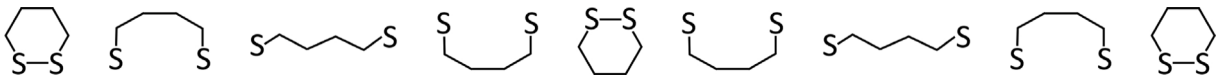

Fig. 3. Schematic of the 'Newton's cradle' type motion observed for photoexcited dithiane in the calculations of Rankine et al. This motion originates on the S_1 state when initiated by a 290 nm photon, but can involve more highly excited states, and results in periodic passage over the extended coupling region between S_1 and S_0 (and other pseudo-degenerate states), offering repeated opportunities for internal conversion and/or intersystem crossing to S_0 and re-formation of the S–S bond on the electronic ground state.

Table 1
Fitting parameters determined from the present work and reported by Stephansen et al.. See text and Eqs. (1) and (2) for parameter definitions.

Parameter	Stephansen et al.	Present work
A_0	–	1.000 ± 0.002
A_1	–	0.033 ± 0.017
A_2	–	0.045 ± 0.005
A_3	–	0.038 ± 0.003
τ_1 /fs	177 ± 17	212 ± 74
τ_2 /ps	2.75 ± 0.23	–
Period, $T = 2\pi/\omega$ /fs	411 ± 27	499 ± 230
ϕ /rad	2.38 ± 0.11	4.49 ± 0.01
FWHM/fs	–	194 ± 26

ground-state dithiane can no longer be ionised efficiently by the probe. This longer-timescale decay was found by Stephansen et al. to have a lifetime of 2.75 ± 0.23 ps.

A few years after publication of Stephansen et al.'s study, Rankine et al. [6] reported results from non-adiabatic multiconfigurational molecular dynamics simulations on dithiane, which led them to refine the interpretation of the internal conversion process observed in the earlier study, and in particular to challenge the earlier assignment of the oscillatory motion to a low-frequency normal mode along the S–S coordinate between the S_1 minimum and the S_1/S_0 conical intersection. Instead, Rankine et al.'s calculations revealed a molecular 'Newton's cradle' (sometimes referred to as a 'molecular clackers') motion (see Fig. 3) that allows photoexcited dithiane to pass periodically over an extended S_1/S_0 coupling region. Their calculations also predicted that this coupling region could be reached as early as ~65 fs after photoexcitation. Our own trajectory surface hopping simulations [25] have considered singlet and triplet states up to S_3, and we find that the 'Newton's cradle' motion is observed on all accessible surfaces (S_0 to S_3 and T_1 to T_4). A number of other states are also pseudo-degenerate in the extended coupling region between S_1 and S_0, offering numerous opportunities for passage back to S_0 from both singlet and triplet excited states.

Based on the above information, we used a custom-written genetic algorithm to fit our time-dependent data $P(t)$ to the following function for $t > 0$ (with $P(t) = A_0$ for $t < 0$):

$$P(t) = A_0 + A_1 e^{-t/\tau_1} + A_2 e^{-t/\tau_2} + A_3(1 - e^{-t/\tau_1})\cos(\omega t + \phi)e^{-t/\tau_2} \quad (1)$$

where the A_i are constants, τ_1 and τ_2 are exponential decay constants as outlined above, and ω and ϕ are the frequency and phase of the oscillatory component of the signal. The fitting function was convoluted with a Gaussian to account for the cross-correlation time before comparison with the experimental data, with the width of the Gaussian able to be included as one of the fitting parameters. Uncertainties on the fitting parameters were determined via a Monte-Carlo procedure in which each fitting parameter was varied in turn while the remaining parameters were held at their best-fit values. Values of the varying parameter for which the fit remained within the experimental uncertainties were retained, and the uncertainty in the fitting parameter was taken as the standard deviation of these 'successful' values.

The full set of best-fit parameters returned from the fit is given in Table 1, together with relevant values from Stephansen et al. [2]. Of most interest, the fit returned values of (212 ± 74) fs for τ_1, (499 ± 230) fs for the oscillation period, and (194 ± 26) fs for the cross-correlation time. The fit was found to be remarkably insensitive to the value of τ_2, as long as it was much longer than the measurement time of ~1 ps. In fact, the fit was improved slightly by setting τ_2 to infinity. We can therefore only conclude that $\tau_2 \gg 1000$ fs. Setting $\tau_2 = \infty$ in Eq. (1) yields a simplified fitting function for $t > 0$:

$$P(t) = A_0 + A_1 e^{-t/\tau_1} + A_2 + A_3(1 - e^{-t/\tau_1})\cos(\omega t + \phi) \quad (2)$$

This simplified fitting function was used to determine the best-fit parameters given in Table 1.

While the best-fit values reported by Stephansen et al. and determined in the present work for τ_1 and the oscillation period T are not identical, they do agree within the stated uncertainties. Considering the different ionisation mechanisms and products detected in the two studies, this implies that the dynamics occurring in photoexcited dithiane leave a common imprint. Discrepancies may arise for a variety of reasons. For example, in the present study we employ strong-field ionisation: generation of multiply charged dithiane by the probe laser is expected to lead to almost instantaneous Coulomb explosion to form the detected S^{2+} fragments. In contrast, the singly charged parent ions formed through multiphoton ionisation in the work of Stephansen et al. are likely to dissociate over a somewhat longer timescale to form the detected $C_4H_7^+$ fragment ions. However, given the similar values measured for τ_1 in the two experiments, the different ionisation mechanisms do not appear to be a major contributing factor to the measured lifetimes.

As noted above, our fits are remarkably insensitive to the lifetime τ_2 for the slowly decaying component of the signal, with the fits favouring the longest possible values. This is in contrast with the lifetime of 2.75 ps determined by Stephansen et al. One could make similar arguments to those above relating to the requirements for forming the detected ions (S^{2+} and $C_4H_7^+$, respectively) in the two different detection schemes, and perhaps the competition between internal relaxation and dissociation of the parent ions, but these would be speculative at best. We do not observe time-dependent behaviour in the small $C_4H_7^+$ signal observed in our experiment. However, the formation mechanism for this ion in our experiment is certainly different from that in the work of Stephansen et al. so this is not necessarily surprising.

To summarise the two sets of results, we can say with some confidence that while the probe schemes, ionisation mechanism, and detected products differ between the two experiments, both probe schemes are sensitive to the same dynamics in the photoexcited parent dithiane molecule.

Our trajectory surface hopping calculations can provide further insight into the relationship between the time-dependent structural changes in dithiane following photoexcitation and the observed time-dependent ion yields in our pump–probe measurements. It is clear from the experimental data that the ionisation probability changes as a function of molecular structure, and therefore as a function of time. At the probe laser intensity employed in our experiment, tunnel ionisation is the primary ionisation mechanism for the structurally evolving dithiane molecule. Since the weakly bound valence electrons will be ionised preferentially when the molecular potential is distorted by the intense laser field, we expect the structure (and therefore time) dependence of the ionisation probability (and therefore the ion yield) to mirror that of the first few ionisation potentials of neutral dithiane. The first three time-dependent ionisation potentials, calculated according to the procedure described in Section 2.2, are shown in Fig. 4. For all three ionisation channels shown, we see strong time-dependent features in the ionisation potentials on the same timescale as those observed in the experimentally measured S^{2+} ion yields. In the cases

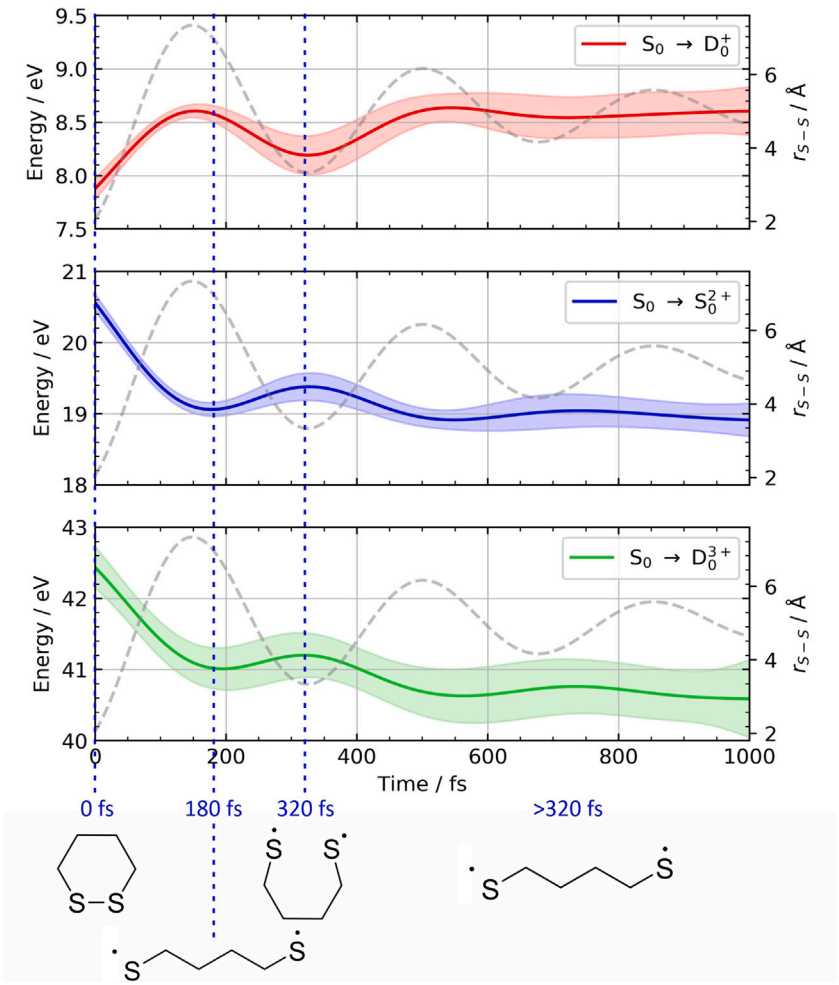

Fig. 4. First, second, and third ionisation potentials of photoexcited 1,2-dithiane calculated as a function of time and averaged over a series of 50 representative trajectories from our trajectory surface hopping simulations. Representative structures at several time points are shown below the plots. To enable comparison with the experimental results, the data have been convoluted with a Gaussian of FWHM 190 fs to account for the cross-correlation time of the pump and probe lasers. The ensemble-averaged S–S bond distance is also shown (dashed line).

of double and triple ionisation to form the dication and trication, respectively, we see an initial rapid decay in the ionisation potential, followed by a longer timescale decay superimposed with an oscillatory component. In contrast, the first ionisation energy shows somewhat different behaviour, with an initial short-timescale rise rather than a decay, and an oscillatory component which is inverted relative to that observed for the other two charge states. The explanation for the inverted behaviour lies in the balance between stabilisation of the cation by overlap of lone pairs on the two sulphur atoms, and electrostatic repulsion between multiple charges in close proximity. In the case of the monocation, lone-pair stabilisation lowers the energy of the cation (and therefore the ionisation potential) at short S–S distances, while for all other charge states this stabilisation is outweighed by electrostatic repulsion, and larger separations are favoured. As noted earlier, the strong-field ionisation probe employed in our experiments yields parent ions in sufficiently high charge states to generate mostly atomic ions as the observed products. It seems reasonable to assume that the ionic ground states for these high charge states are all strongly repulsive, and therefore that the ionisation energies from neutral dithiane to these multiply charged states will behave in a similar way to those for the double and triple ionisation energies shown in Fig. 4.

In conclusion, we have shown that when using strong-field-induced Coulomb explosion to probe the products of a photoexcitation process, the time-dependent ion yields are sensitive to the evolving molecular structure. Applied to the 290 nm photoexcitation dynamics of 1,2-dithiane, this approach reveals dynamics very similar to those observed previously by Stephansen et al. using a multiphoton single-ionisation probe scheme. Our observations are consistent with previous experimental [2,3] and theoretical [5–8] studies, revealing ultrafast stretching of the S–S bond on the S_1 excited electronic surface, followed by oscillatory dynamics that periodically allow population to pass through the S_1/S_0 conical intersection to the ground electronic surface, where the S–S bond is able to re-form. The present study paves the way for more detailed Coulomb-explosion imaging studies with the potential to achieve direct visualisation of the ultrafast photoinduced dynamics in dithiane.

CRediT authorship contribution statement

Patrick A. Robertson: Writing – review & editing, Writing – original draft, Project administration, Methodology, Investigation, Funding acquisition, Formal analysis, Conceptualization. **James Merrick:** Writing – review & editing, Investigation, Conceptualization. **David Heathcote:** Writing – review & editing, Investigation, Formal analysis, Data curation. **Matthew S. Robinson:** Writing – review & editing, Methodology, Investigation, Formal analysis, Data curation. **Alexander Butler:** Writing – review & editing, Investigation. **Yasmine Biddick:** Writing – review & editing, Methodology, Investigation. **J.F. Pedro Nunes:** Writing – review & editing, Investigation. **Conor Rankine:** Writing – review & editing, Investigation. **Zhihao Liu:** Writing – review & editing,

Investigation. **Samuel F. Arrowsmith:** Writing – review & editing, Investigation. **James O.F. Thompson:** Writing – review & editing, Resources, Methodology, Investigation. **M. Nrisimha Murty:** Writing – review & editing, Investigation. **Richard Chapman:** Writing – review & editing, Resources, Investigation. **Emma Springate:** Writing – review & editing, Resources, Project administration, Investigation. **Edward A. Anderson:** Writing – review & editing, Investigation, Conceptualization. **Adam Kirrander:** Writing – review & editing, Methodology, Investigation, Conceptualization. **Claire Vallance:** Writing – review & editing, Writing – original draft, Supervision, Resources, Project administration, Methodology, Investigation, Funding acquisition, Formal analysis, Data curation, Conceptualization.

Declaration of competing interest

The authors declare that they have no known competing financial interests or personal relationships that could have appeared to influence the work reported in this paper.

Acknowledgements

We would like to thank the staff at the UK Central Laser Facility, and in particular the Artemis ultrafast laser team, for access to the Artemis facility and for their support during our beamtime. We would also like to thank Basile Curchod and Dennis Milesevic for helpful discussions. This work was funded primarily via EPSRC Programme Grants EP/V026690/1 and EP/T021675/1. In addition, JM acknowledges funding via an EPSRC doctoral studentship and the Carolyn and Franco Gianturco Theoretical Chemistry Scholarship from Linacre College, Oxford. AK acknowledges funding from the Engineering and Physical Sciences Research Council (EPSRC) grants EP/V006819/2, EP/V049240/2, EP/X026698/1, EP/X026973/1, and the U.S. Department of Energy, Office of Science, Basic Energy Sciences, under award number DE-SC0020276, with further support from the Leverhulme Trust *via* grant RPG-2020-208. MR acknowledges funding from the Cluster of Excellence "Advanced Imaging of Matter" of the Deutsche Forschungsgemeinschaft (DFG)(AIM, EXC 2056, ID 390715994).

Data availability

Data will be made available on request.

References

[1] O. Mozziconnaci, K.B. A., C. Schönieich, Photolysis of an intrachain peptide disulfide bond: primary and secondary processes, formation of H_2S, and hydrogen transfer reactions, J. Phys. Chem. B 114 (2010) 3668–3688.

[2] B.A. Stephansen, R.Y. Brogaard, T.S. Kuhlman, L.B. Klein, J.B. Christensen, T.I. Sølling, Surprising intrinsic photostability of the disulfide bridge common in proteins, J. Am. Chem. Soc. 134 (2012) 20279–20281.

[3] M.A.B. Larsen, A.B. Skov, C.M. Clausen, J. Ruddock, B. Stankus, P.M. Weber, T.I. Sølling, Putting the disulfide bridge at risk: How UV-C radiation leads to ultrafast rupture of the S-S bond, Chem. Phys. Chem. 19 (2018) 2829–2834.

[4] H.G. McGhee, R. Totani, O. Plekan, M. Coreno, M. de Simone, A. Mumtaz, S. Singh, B.C. Schroeder, B.F.E. Curchod, R. Ingle, Core and valence photoelectron spectroscopy of a series of substituted disulfides, J. Chem. Phys. 161 (2024) 134303.

[5] C. Middleton, C.D. Rankine, T.J. Penfold, An on-the-fly deep neural network for simulating time-resolved spectroscopy: predicting the ultrafast ring opening dynamics of 1,2-dithiane, Phys. Chem. Chem. Phys. 25 (2023) 13325–13334.

[6] C.D. Rankine, J.P.F. Nunes, M.S. Robinson, P.D. Lane, D.A. Wann, A theoretical investigation of internal conversion in 1,2-dithiane using non-adiabatic multiconfigurational molecular dynamics, Phys. Chem. Chem. Phys. 18 (2016) 27170–27174.

[7] Y. Lassmann, D. Hollas, B.F.E. Curchod, Extending the applicability of the multiple-spawning framework for nonadiabatic molecular dynamics, J. Phys. Chem. Lett. 13 (2022) 12011–12018.

[8] L.M. Ibele, Y. Lassmann, T.J. Martínez, B.F.E. Curchod, Comparing (stochastic-selection) ab initio multiple spawning with trajectory surface hopping for the photodynamics of cyclopropanone, fulvene, and dithiane, J. Chem. Phys. 154 (2021) 104110.

[9] J. Cao, D.-C. Chen, Disulfide bond photochemistry: the effects of higher excited states and different molecular geometries on disulfide bond cleavage, Phys. Chem. Chem. Phys. 21 (2019) 4176–4183.

[10] H. Yuan, Y. Gao, B. Yang, S. Gu, H. Lin, D. Guo, J. Liu, S. Zhang, X. Ma, S. Xu, Coulomb explosion imaging of complex molecules using highly charged ions, Phys. Rev. Lett. 133 (2024) 193002.

[11] C.A. Schouder, A.S. Chatterley, J.D. Pickering, H. Stapelfeldt, Laser-induced Coulomb explosion imaging of aligned molecules and molecular dimers, Ann. Rev. Phys. Chem. 73 (2022) 323–347.

[12] X. Li, M.S. Rudenko, N. Anders, T.M. Baumann, S. Eckart, B. Erk, A. De Fanis, K. Fehre, R. Dörner, L. Foucar, S. Grundmann, P. Grychtol, A. Hartung, M. Hofmann, M. Ilchen, C. Janke, G. Kastirke, M. Kircher, K. Kubicek, M. Kunitski, T. Mazza, S. Meister, N. Melzer, J. Montano, V. Music, G. Nalin, Y. Ovcharenko, C. Passow, A. Pier, N. Rennhack, J. Rist, D.E. Rivas, I. Schlichting, L.P.H. Schmidt, P. Schmidt, J. Siebert, N. Sternger, D. Trabert, F. Trinter, I. Vela-Perez, R. Wagner, P. Walter, M. Weller, P. Ziolkowski, A. Czasch, D. Rolles, M. Meyer, T. Jahnke, R. Boll, Coulomb explosion imaging of small polyatmoic molecules with ultrashort X-ray pulses, Phys. Rev. Res. 4 (2022) 013029.

[13] S.W. Crane, J.W.L. Lee, M.N.R. Ashfold, D. Rolles, Molecular photodissociation dynamics revealed by Coulomb explosion imaging, Phys. Chem. Chem. Phys. 25 (2023) 16672–16698.

[14] Z. Vager, R. Naaman, E.P. Kanter, Coulomb explosion imaging of small molecules, Sci. 244 (1989) 426–431.

[15] R. Boll, J.M. Schäfer, B. Richard, K. Fehre, G. Kastirke, Z. Jurek, M.S. Schöffler, M.M. Abdullah, N. Anders, T.M. Baumann, S. Eckart, B. Erk, A.D. Fanis, R. Dörner, S. Grundmann, P. Grychtol, A. Hartung, M. Hofmann, M. Ilchen, L. Inhester, C. Janke, R. Jin, M. Kircher, K. Kubicek, M. Kunitski, X. Li, T. Mazza, S. Meister, N. Melzer, J. Montano, V. Music, G. Nalin, Y. Ovcharenko, C. Passow, A. Pier, N. Rennhack, J. Rist, D.E. Rivas, D. Rolles, I. Schlichting, L.P.H. Schmidt, P. Schmidt, J. Siebert, N. Strenger, D. Trabert, F. Trinter, I. Vela-Perez, R. Wagner, P. Walter, M. Weller, P. Ziolkowski, S.-K. Son, A. Rudenko, M. Meyer, R. Santra, T. Jahnke, X-ray multiphoton-induced Coulomb explosion images complex single molecules, Nat. Phys. 18 (2022) 423–428.

[16] Central Laser Facility (STFC), Atomic and molecular physics, 2024, URL https://www.clf.stfc.ac.uk/Pages/Atomic-and-molecular-physics.aspx. (Accessed 28 December 2024).

[17] R. Singh, G.M. Whitesides, Degenerate intermolecular thiolate-disulfide interchange involving cyclic five-membered disulfides is faster by approximately 10^3 than that involving six-or seven-membered disulfides, J. Am. Chem. Soc. 112 (1990) 6304–6309.

[18] J.C. Tully, Molecular dynamics with electronic transitions, J. Chem. Phys. 93 (1990) 1061–1071.

[19] M. Oppel, Sharc-md/sharc: SHARC release 2.1.2, 2022, Software URL https://github.com/sharc-md/sharc.

[20] S. Mai, P. Marquetand, L. González, Nonadiabatic dynamics: The SHARC approach, Wiley Interdiscip. Rev. Comput. Mol. Sci. 8 (2018) e1370.

[21] M. Richter, P. Marquetand, J. González-Vázquez, I. Sola, L. González, SHARC: Surface hopping including arbitrary couplings — program description and benchmarking, J. Chem. Theory Comput. 7 (2011) 1253–1258.

[22] G.L. Manni, I.F. Galván, A. Alavi, et al., Multiconfiguration approaches for strong electron correlation in chemistry, J. Chem. Theory Comput. 19 (2023) 6933–6991.

[23] B.O. Roos, P.R. Taylor, P.E. Sigbahn, A complete active space SCF method (CASSCF) using a density matrix formulated super-CI approach, Chem. Phys. 48 (1980) 157–173.

[24] J.P. Zobel, P.-O. Widmark, V. Veryazov, Automatic selection of active space for multiconfigurational calculations, J. Chem. Theory Comput. 16 (2020) 278–294.

[25] J. Merrick, C. Vallance, A. Kirrander, Triplets in the cradle: the curious case of 1,2-dithiane, Prep. Phys. Chem. Chem. Phys. (2024).